

Corrosion behavior of Ni/Al₂O₃ and Ni/ZrO₂ nanocomposite thin films

C. GHEORGHIES*, I. V. STASI, C. C. LALAU

Faculty of Mechanics, Dunarea de Jos University of Galati, Domnesca str., no.47, code RO800008, Romania

The addition of alumina and zirconia nanoparticles into nickel plating bath induces changes in the surface morphology and in the preferred crystallographic orientation of the nanocomposite thin layers electrodeposited on copper substrates. The typical morphology for nickel deposits is pyramidal, but the addition of alumina particles in concentrations between 5 g/l and 10 g/l changes this morphology to hemispherical. The behavior of prepared Ni/Al₂O₃ and Ni/ZrO₂ nanocomposite thin layers during corroding process in various solutions was investigated by using polarization curve, impedance spectroscopy, and Mott-Schottky techniques. The experimental results indicate the beneficial roles of alumina and zirconia nanoparticles on nanocomposite materials.

(Received February 6, 2009; after revision February 8, 2009; accepted February 25, 2009)

Keywords: Nickel matrix composites, Nanoparticles, Corrosion

1. Introduction

This paper investigates the effects of adding alumina and zirconia nanoparticles in the electrolyte bath on surface morphologies and structure of electrodeposited nickel, and their subsequent influence on the corrosion process in various solutions. These results are important for the fabrication of thermal and corrosion barriers by means of covering metallic surfaces with protective layers.

2. Nanocomposite preparation

The electrodeposition process and corrosion studies have been performed on the same electrochemical cell. The corrosion process was monitored in a corrosion cell consisting of a round-bottomed flask, platinum auxiliary electrodes, and a standard calomel electrode serving as the reference electrode.

The applied potential and resulting current were measured by a VOLTALAB 10 potentiostat/galvanostat and with a typical corrosion measurement software from RADIOMETER ANALYTICAL SAS Company.

The general view of experimental arrangement in Fig. 1 is shown. The temperature of the used solutions were controlled when placing the electrochemical cell in TK-1 thermostat.

On copper support, we have deposited 10 nanocomposite layers, in a nickel matrix, with ZrO₂ particles (6-8 nm) and 7 specimens having similar matrix with Al₂O₃ particles (20 nm) [1, 2]. We also created 3 specimens with simple nickel deposition in order to compare their behavior with the version with nanoparticles.

The support specimens have been properly prepared for deposition, using specific solutions for degreasing, pickling and activation of surfaces. For the electrolyte solution, a Watt bath was used having the following features: NiSO₄·6H₂O-0.90M; NiCl₂·6H₂O-0.20M; H₃BO₃-0.28M; sodium dodecylsulphate [CH₃(CH₂)₁₁OSO₃Na]-0.4 g/l [3].



Fig.1 Voltalab 10 equipment for electrodeposition and corrosion measurements

The pH value of the solution was maintained at 4.2 – 4.5 and the corrections were made using an acidic solution.

The concentration of zirconia was 10 g/l and concentration of alumina varied from 0 to 20 g/L. Both types of nanoparticles were kept in suspension by a magnetic stirrer.

The stirring rate of the plate agitator was 700 rpm. Firstly, the supports are decreased for 15-20 minutes in a solution and then wiped with a filter paper. Secondly, the specimen is introduced in the pickling solution (HNO₃ 20%) and thoroughly rinsed distilled water. We noticed that the surface shows metallic lustre and the wash with distilled water creates a uniform film. Thirdly, the specimen is introduced in an activating solution (H₂SO₄50%) and washed again with distilled water. Finally, it is rapidly introduced in the electrolysis bath containing the prepared electrolyte solution. Before weighting them on a precision balance, the specimens need to be thoroughly dried.

Depositions were made at an optimal temperature of 40° C for 90 minutes and a current density of 2A/dm². The cathode consisted of the working specimen and the anode consisted of pure nickel with the same surface area as the specimen. After 90 minutes, the electric power was disconnected and electrodes were removed from the bath. The specimens with composite deposition were washed

with plenty of distilled water. After the specimens dries, they are weighed on the precision balance to compute the actual deposited quantity.

The main tools used for the surface characterization for nanocomposite layers were scanning electron microscopy (SEM) equipped with an EDAX, and X-ray diffractometer (XRD). The OLYMPUS PM3 microscope allows for morphological observations of the microstructure. The analysis by XRD shows that only some planes common to nickel system are expected and these are presented in Table 1.

Table 1. Planes of nickel system.

(hkl)	2θ (°)	I (a.u.)
111	44.51	100
200	51.85	42
220	76.37	21
311	92.94	20

3. Structural analysis

The obtained electrodeposited layers of nickel having alumina or zirconia nanoparticles were studied by scanning electron microscopy at different magnifications. It is important to choose the optimal magnifications to obtain the best images in which some agglomeration of nanoparticles in the electrodeposited layers can be observed.

If a cross section is made in the resulted nanomaterial, it is possible to observe different thicknesses of the electrodeposited layer. This thickness depends of current density, the deposited time and other variable of electrodeposition process (e.g. nanoparticles composition). The effect of nanoparticles on thickness can be explained by the growth of the agglomerating particles in the layers that become bigger when higher amounts of particles are present [4].

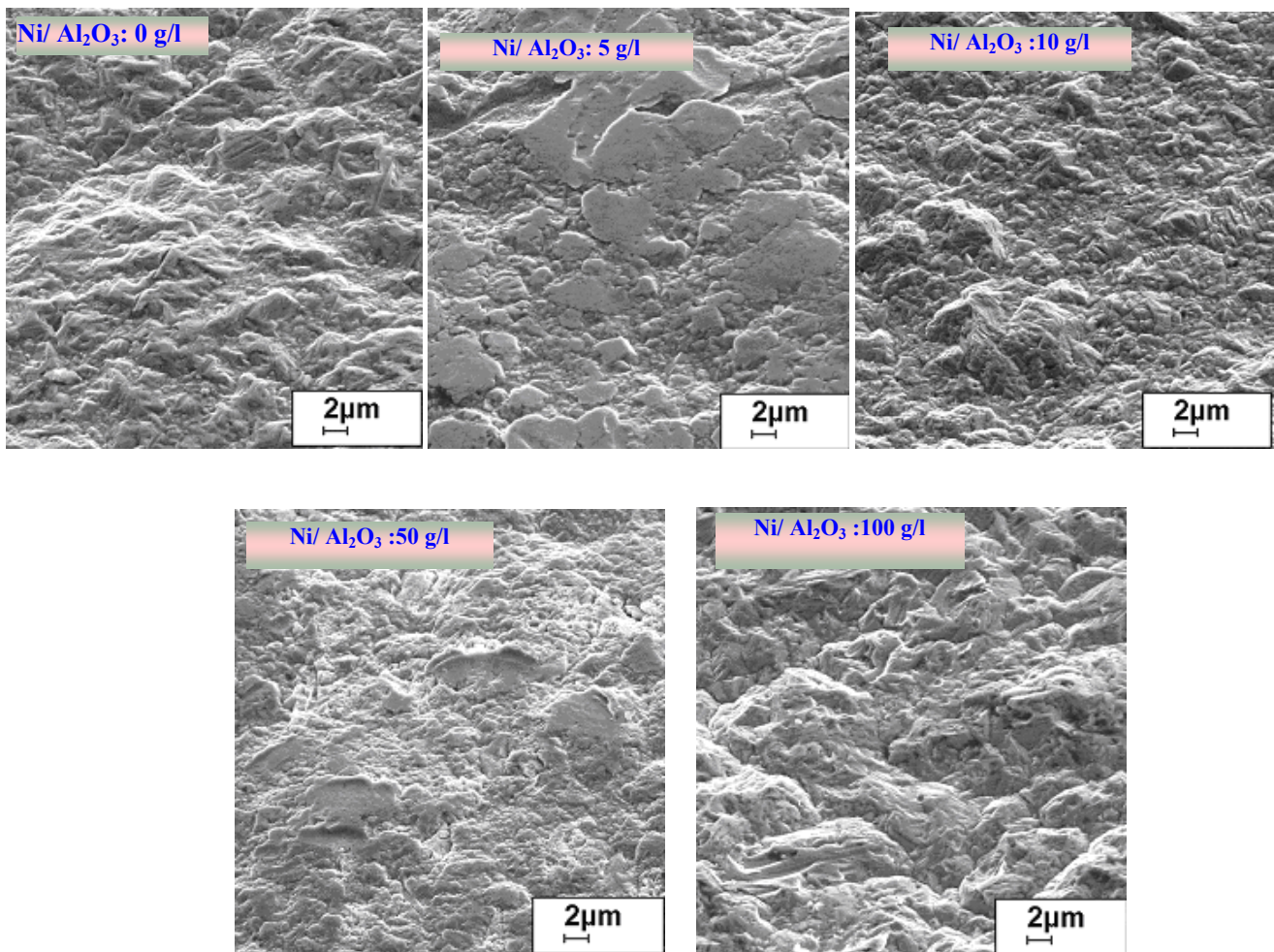


Fig.2. SEM images of Ni/Al₂O₃ surface.

In Fig. 2 SEM images of Ni/Al₂O₃ electrodeposition are displayed for five different alumina nanoparticles concentrations reaching to 10g/l.

As alumina was added to the electrolyte in increasing concentrations, a general refinement in the grain structure on the surface is observed. With addition of 5 g/l of

alumina, the average size of the pyramids on the surface is clearly reduced [5]. There is also a reduction in the surface grain size to micrometer and sub micrometer grains. These results show that the surface morphology is greatly refined by the presence of alumina in the bath for the coatings deposited at 2 A.dm⁻².

The chemical analysis of electrodeposited layer with alumina nanoparticles has been estimated by EDAX method. The typical spectrum showing the chemical construction is presented in Fig. 3.

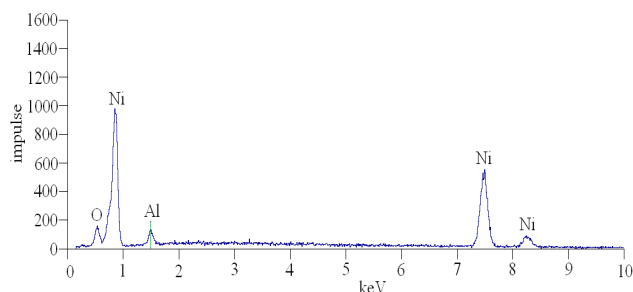


Fig. 3. EDAX spectrum of electrodeposited film with alumina nanoparticles.

X-ray pattern from an electrodeposited film of nickel having a concentration of 10 % alumina nanoparticles is presented in Fig. 4. Although EDAX spectra pointed out aluminum, only the characteristic peaks of nickel can be observed.

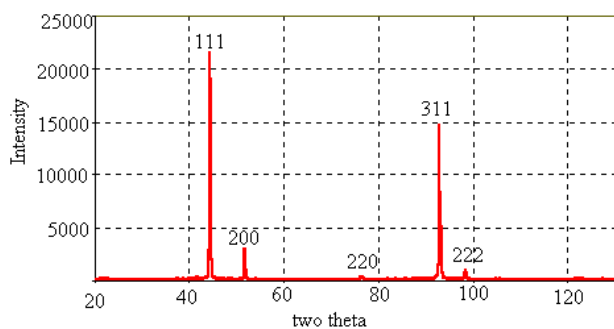


Fig. 4. X-ray diffraction pattern of electrodeposited nickel film with 10 % alumina nanoparticles.

The thin films of nickel which were obtained with zirconia nanoparticles present in the electrolyte had an uniform white-silvery appearance. To obtain a reference for the determination of deposition efficiency, three pure nickel depositions were first conducted.

In theory, should have been deposited 8.21g/dm^2 , while experiments showed a deposit of 7.8241g/dm^2 . Nickel weight deposited on the specimen was $m_{\text{experimental}} = 0.3129\text{ g}$ and $m_{\text{theoretical}} = 0.3284\text{ g}$. Achieved efficiency was $\eta = 95.30\%$ i.e. an optimum deposition efficiency over 95%, typical for nickel depositions in an electrolytic bath of sulfate-chloride; in a Watt's bath, 97.5% efficiency is obtained. Average weight of nickel with ZrO_2 deposited on the specimen is $m_{\text{experimental}} = 0.2822\text{ g}$. From $m_{\text{theoretical}}$ and $m_{\text{experimental}}$, efficiency can be deduced as $\eta = 85.94\%$.

Pure nickel depositions were obtained with an efficiency of more than 95.30%. On the other hand, in the experiments performed for composite depositions, a

smaller efficiency was achieved due to the presence of ZrO_2 particles. One possible explanation is that in the paths followed by the Ni^{2+} ions to the cathode and that of the anions to the anode, ZrO_2 particles in the suspension may slow the nickel reduction process. Moreover, ZrO_2 particles can be found in the deposits, and there is an equilibrium between the forces keeping the particles down in the deposition and those existing in the suspension. This situation is not yet fully understood for a composite deposition mechanism.

4. Corrosion tests

Corrosion tests have been performed for composite coating specimens of Ni/ZrO_2 in three different types of solvents: NaCl 3%, Na_2SO_4 0.1M and H_2SO_4 0.1N. The results were compared with depositions of metallurgical nickel. The Na_2SO_4 0.1 M solution is an electrolyte who has the advantage of being inert over most of the other tested materials, and the 0.1 M concentration ensures the appropriate conductivity for the three electrochemical studies that were performed: polarization curve, EIS spectroscopic impedance, and Mott-Schottky spectroscopic impedance [2].

Previously, we isolated with nylon (polytetrafluoroethylene) the surface not subjected to electrochemical tests. Out of the deposited coating (Ni/ZrO_2) area of 4 cm^2 , an area of $0.5\text{--}1\text{ cm}^2$ was reserved for the electrochemical experiments, polarization curves and spectroscopic impedance.

The electrochemical cell used for the electrochemical tests consisted of a glass recipient with a cap having a series of apertures through which we inserted the solution to be analyzed, the working electrode [deposition specimen obtained on the copper support], the auxiliary electrode [helical platinum (Pt) wire] and the referential electrode [horn mercury electrode $\text{Hg}/\text{HgCl}_{2\text{sat}}$. ($\epsilon = 0.234\text{ V}$)]. The solution was stirred by introducing a small magnet covered by a nylon or glass layer, which was then moved a magnetic stirrer.

Nickel specimens with zirconium oxide particles have been studied against pure nickel specimens. Initially, polarization curves were achieved in the previously mentioned electrolyte solutions (NaCl 3%, Na_2SO_4 0.1M and H_2SO_4 0.1N). Then we observed the behavior of the Ni/ZrO_2 depositions and that of the metallurgical nickel specimen.

The working circuit consisted of: referential electrode: horn mercury, auxiliary electrode: platinum and working electrode: deposition in nickel matrix. This circuit was connected to a computer which recorded the experimental data. The polarization curves $i = f(E)$ were obtained in the following conditions: voltage 0: -500 mV ; voltage 1: $+500\text{ mV}$; voltage 2: $+1000\text{ mV}$; sweeping speed (rate) $v = 150\text{ mV/min}$; number of cycles: 1, minimum current: -50 mA and maximum current: $+50\text{ mA}$. Figs. 5-7 contain these polarization curves, and the corresponding numerical values are synthetically reported in Table 2.

Table 2. Experimental data obtained from polarization curves.

	Ni	Ni/ZrO ₂	Ni	Ni/ZrO ₂	Ni	Ni/ZrO ₂
	Na ₂ SO ₄ 0.1 M		NaCl 3%		H ₂ SO ₄ 0.1 N	
E (i=0) (mV)	-321.1	-131.3	-237.1	-232.2	-257.9	-257.9
R _p (kΩ·cm ²)	16.41	104.54	7.85	20.98	126.63	126.63
i _{cor} (μA/cm ²)	0.9583	0.0693	1.299	0.229	0.0909	0.0909
v _{cor} (mm/year)	0.013	0.001	0.018	0.003	1.243	1.243
A (cm ²)	7.9	0.6	8.69	0.72	8.69	0.54

Key: E – voltage; i_{cor} – corrosion intensity; R_p – polarization resistance; v_{cor} – corrosion rate; A – surface area

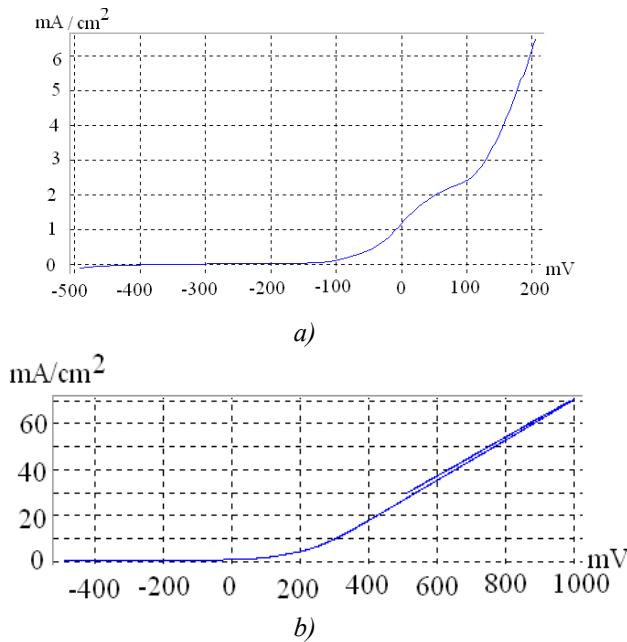


Fig. 5. Polarization curves: a) Ni in NaCl 3% solution, b) Ni/ZrO₂ in NaCl 3% solution

The obtained curves and the rates of corrosion indicate that the voltage is shifted to higher positive values for composite coatings of Ni/ZrO₂ (-232.2 mV for NaCl 3% solution; -131.3 mV for Na₂SO₄ 0.1M solution) against the metallurgical nickel (-237.1 mV for NaCl 3% solution; -321.1 mV for Na₂SO₄ 0.1M solution) and against the initial voltage, - 500 mV. In H₂SO₄ 0.1N solution, the voltage is found as being the same (-257.9 mV). The highest positive potential (-131.3 mV) was obtained for composite coatings of Ni/ZrO₂ in Na₂SO₄ 0.1M solution. A significant decrease in voltage occurs for the Ni/ZrO₂ specimens in Na₂SO₄ 0.1 M electrolyte, of approximately 200mV decrease. For the other electrolytes, no significant changes between the composite depositions and pure Ni were recorded.

The highest change in polarization resistance compared with pure Ni is obtained for Ni/ZrO₂ composite deposition in a Na₂SO₄ 0.1 M electrolyte. Correlated with this parameter, the corrosion intensity is the lowest on the same specimens, respectively 0.0693 (μA/cm²) for a polarization resistance of 104.54 (Kohm·cm²). The higher corrosion resistance and smaller the corrosion intensity are, the more resistant is the specimen to the destruction process.

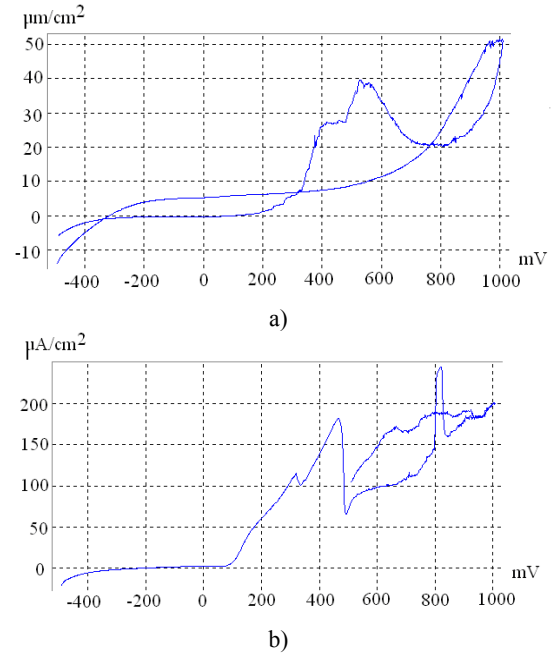


Fig. 6. Polarization curve: a) Ni in Na₂SO₄ 0.1 M solution, b) Ni/ZrO₂ in Na₂SO₄ 0.1 M solution

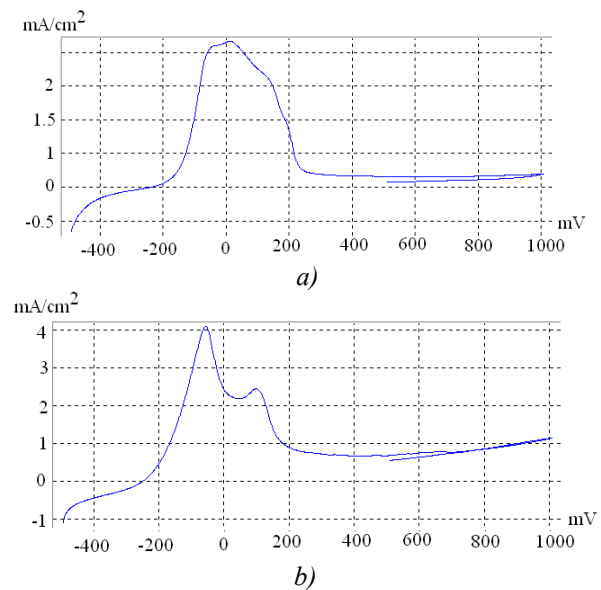


Fig. 7. Polarization curve: a) Ni in H₂SO₄ 0.1 N solution, b) Ni/ZrO₂ in H₂SO₄ 0.1 N solution

In table 3 the corrosion rates are listed, expressed in mm/year. The lowest value was obtained for Ni/ZrO₂ composite deposition in Na₂SO₄ 0.1 M electrolyte (0.001 mm/year) and the second lowest one for NaCl 3% (0.003 mm/year).

Table 3. Experimental data on spectroscopic impedance research.

t(min.)	10	45	60	70	85	90	120	140
E(V)	0.18	0.15	0.15	0.15	0.14	0.13	0.11	0.1
t(min.)	180	200	240	1440	2670	2735	2790	2820
E(V)	0.09	0.09	0.08	0.09	0.1	0.09	0.02	0

In the H_2SO_4 0.1 N electrolyte, which is highly acidic, the parameters for specimens studied by comparison are identical, thus polarization curve research in this electrolyte does not provide analytical information.

In conclusion, the determination of the polarization curve must be performed in a proper electrolyte, to maximize the amount of information useful for research. For the studied specimens it was proved that Na_2SO_4 , which is an inert electrolyte which resulted from a tough acid and a tough base, is the most appropriate for the study of polarization curves. Ni/ZrO_2 composite deposition specimens show significantly improved parameters (R_p and i_{cor}) compared with metallurgical Ni.

In Fig. 8, the overlapping of two polarization curves is shown: Ni/ZrO_2 in Na_2SO_4 0.1 M solution and Ni/ZrO_2 in NaCl 3% solution. The two curves cross at: on voltage E_e (-300 mV, -200 mV) and a corrosion rate $i_{\text{cor}} = 0 \mu\text{A}/\text{cm}^2$.

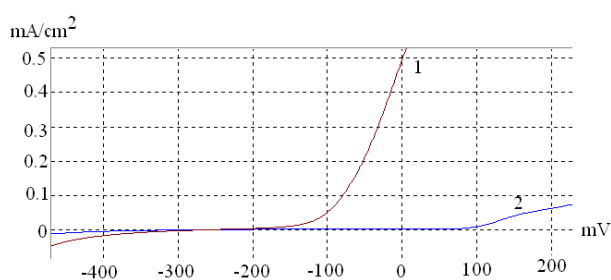


Fig. 8. Polarization curves – Overlapping: Ni/ZrO_2 in Na_2SO_4 0.1 M solution (1), Ni/ZrO_2 in NaCl 3% solution (2).

In Fig. 9, the polarization curve is shown for nickel and Ni/ZrO_2 specimens in H_2SO_4 0.1 N solution. The curve for nickel has a maximum peak at a voltage E_e (7mV, 14 mV) and a corrosion rate i_{cor} (2.150 $\mu\text{A}/\text{cm}^2$, 2.154 $\mu\text{A}/\text{cm}^2$). For Ni/ZrO_2 two maximum peaks are present at a voltage E_{1e} (-65 mV, -55 mV), a corrosion rate $i_{\text{cor}1}$ (4 $\mu\text{A}/\text{cm}^2$, 4.2 $\mu\text{A}/\text{cm}^2$), and at a voltage E_{2e} (80 mV, 100 mV), with a corrosion rate $i_{\text{cor}2}$ (2.3 $\mu\text{A}/\text{cm}^2$, 2.5 $\mu\text{A}/\text{cm}^2$).

In addition, we juxtaposed the polarization curves for Ni/ZrO_2 in H_2SO_4 0.1 N solution (1), and Ni in H_2SO_4 0.1 N solution (2). Both curves have a peak in the same voltage range: E_e (-255 mV, 200 mV).

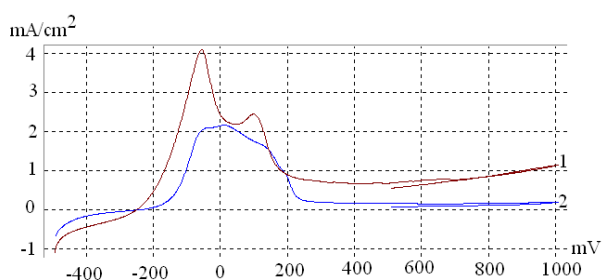


Fig.9. Polarization curves: Ni/ZrO_2 in H_2SO_4 0.1 N solution (1), Ni in H_2SO_4 0.1 N solution (2) – Overlapping.

For composite coatings like nickel – zirconium oxide, compared to nickel coatings, polarization curves have almost the same rates, but shifted to an increased voltage, proving that these composite coatings have better resistance to corrosion.

The corrosion protection can be attributed to the presence of ZrO_2 particles in nickel matrix, because their presence on the metal surface creates a barrier for oxygen reduction. In solutions, the composites are not stable. It is possible to selectively dissolve the metallic matrix or the disperse phase or both (matrix-disperse phase).

Corrosion processes are essentially electrochemical processes and voltage and current parameters can be accurately measured with modern equipment. For the corrosion study, polarization resistances can be evaluated from spectro-electrochemical impedance data (EIS) in a large frequency range ($10^3 - 10^{-3}$ Hz). A voltage change indicates a corresponding change of intermediate species concentration.

The spectroscopic impedance measurements were performed on composite specimens, nickel with zirconium oxide (Ni/ZrO_2) particles in Na_2SO_4 solution, as working electrolyte for the electro-chemical cell. This way, the behavior of the layer deposited in the electrolytic solution was traced during a period of time, to evaluate the parameters.

The working equipment contains a two component circuits: the main and secondary circuits. The main circuit consists of: referential electrode: horn mercury (connected to white color); auxiliary electrode: platinum (connected to red and orange colors) and working electrode: specimen (connected to green and blue colors). The secondary circuit is realized by a salt bridge connecting the referential electrode to the working electrode [6]. The salt bridge prevents contamination of saturated KCl solution from the horn mercury electrode with impurities coming from the solution to be analyzed. To measure the voltage in horn mercury, a voltmeter was introduced in the circuit, with a lug to referential electrode and one to the working one. This circuit is connected to computer and data for electrochemical analysis are recorded.

Specimens undertaking the experiments have been evaluated for certain time spans. The value of voltmeter-measured voltage is reported during the entire electrochemical analysis. Results are rendered in Table 3, and diagram $E = f(t)$ is rendered in Fig. 11. From the spectroscopic impedance measurements, an evaluation can be made by comparing the differences between the measuring voltage values depending on time, as presented in Table 3. The voltages can provide insight into the strength of the coating.

From Fig. 10 shows that voltage changes with time, and a constant voltage drop is recorded from 180 mV to 0 mV during 47 hours. Additional data is presented in Figs 11-12, rendered as Bode and Nyquist charts. Bode chart is usually useful to physicists, while Nyquist chart is preferred by chemists. The impedance measurements on various frequencies can provide full information on the electrochemical system, which gives a particular value to this technique [6,7].

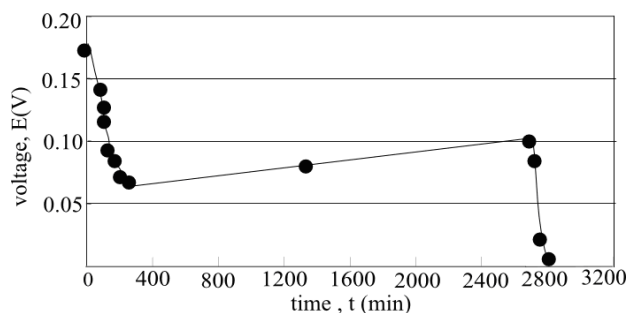


Fig.10. Voltage variation on time

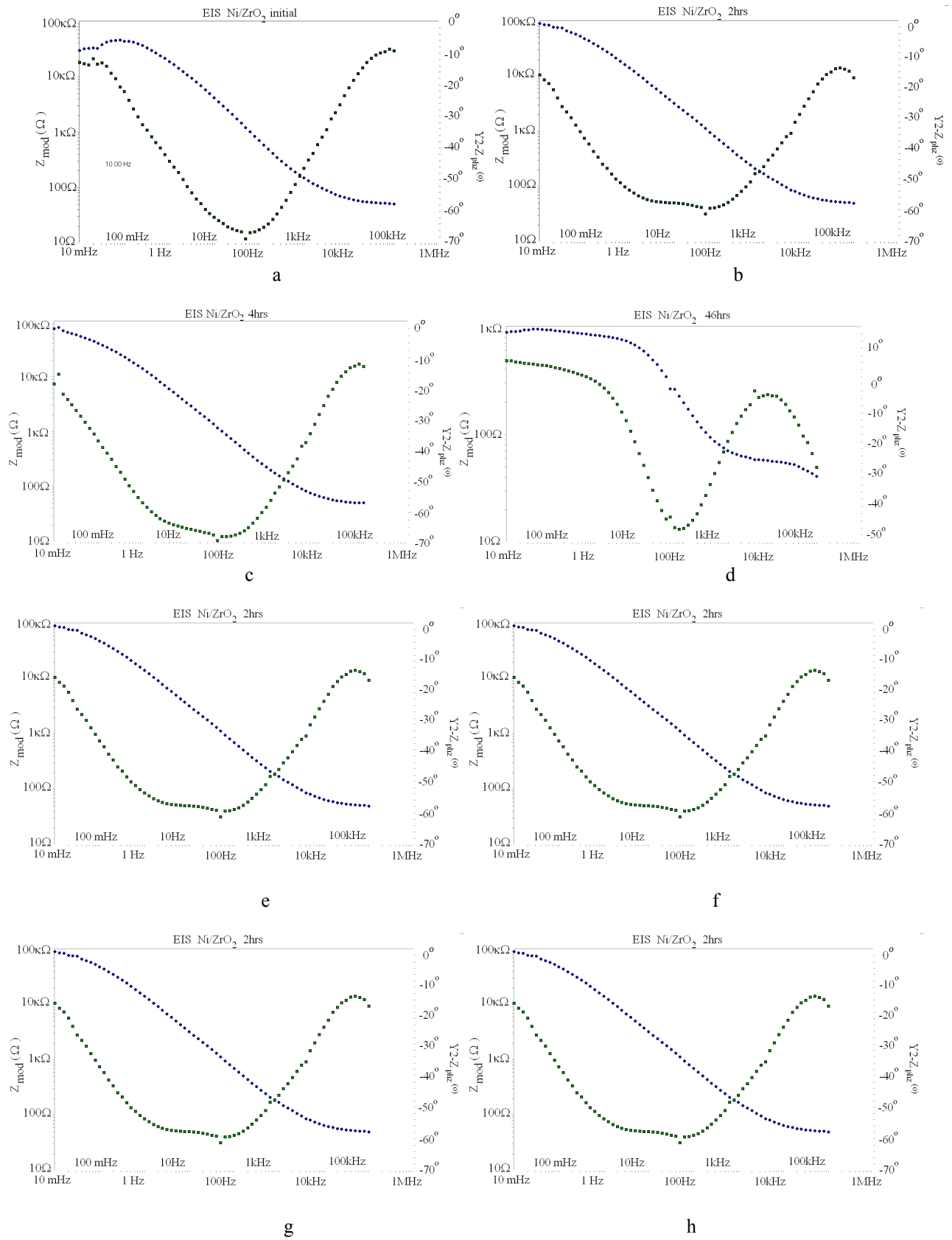


Fig. 11. Representation of Impedance Spectroscopy (BODE Diagram) for the experimental system of Ni/ZrO₂ in Na₂SO₄ 0.1 M solution at $t = 0$ s(a), 1h(b), 2 hrs(c), 3h(d), 4 hrs(e), 24h(f), 46 hrs(g), 47h(h).

Fig. 12 shows that Ni/ZrO₂ composite system has a high polarization resistance, with a maximum of 40 Kohm for a high frequency. After 46 hours Nyquist diagram shows a small 300 ohm polarization resistance, and a small decrease of polarization resistance with time. This

suggests that the presence of zirconium oxide in the deposition may cause load transfer, since this substance can act as activator for the cathode reduction process of the metal.

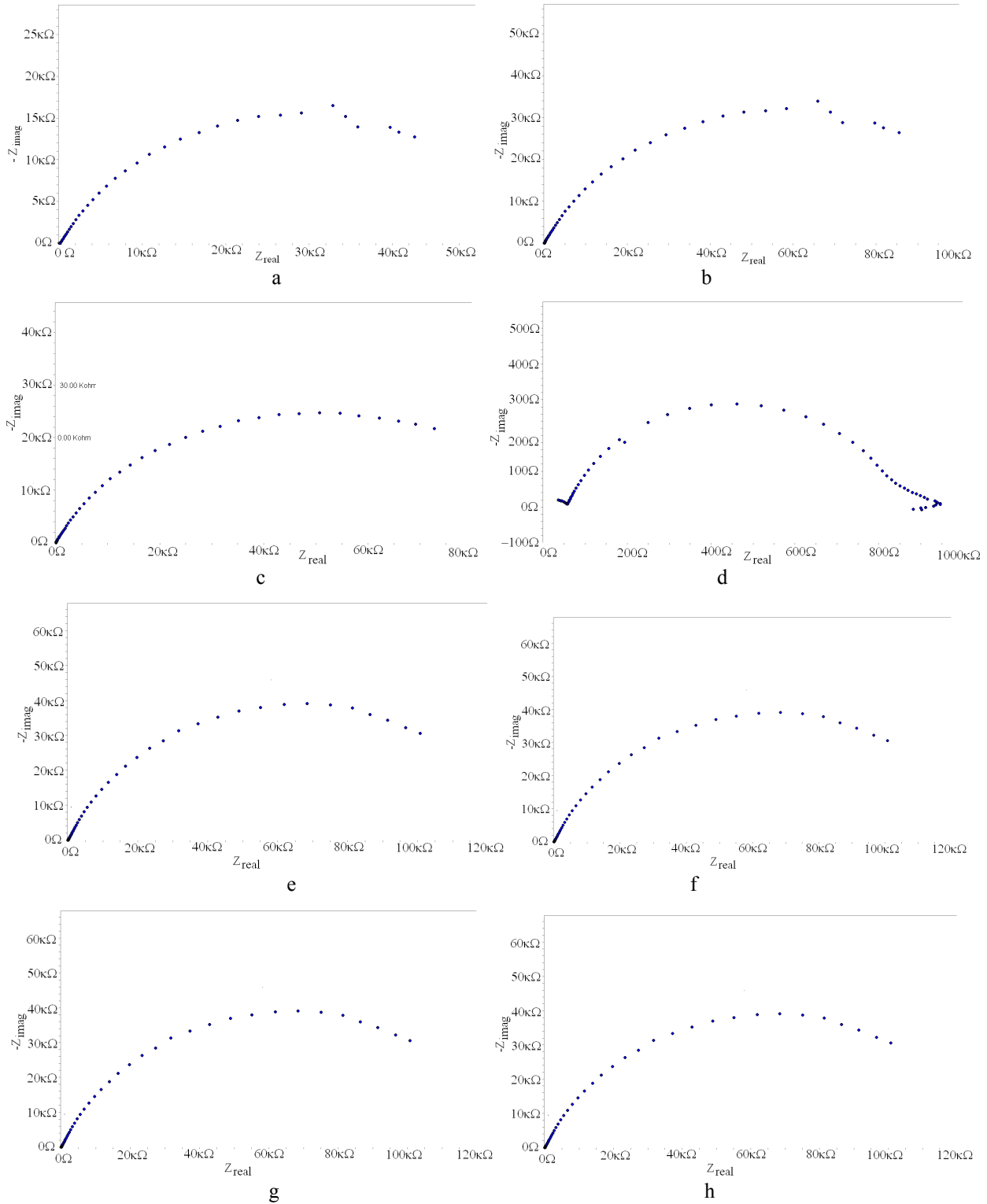


Fig. 12. Representation of Impedance Spectroscopy (Nyquist diagram) for the experimental system of Ni/ZrO₂ in Na₂SO₄ 0.1 M solution at $t = 0$ s (a), 1h(b), 2 hrs(c), 3hrs(d), 4 hrs(e), 24hrs (f), 46 hrs(g), 47hrs(h).

A specimen of Ni/ZrO₂ composite deposition was subjected to Mott Schottky approach, which is a variant of Spectroscopic Impedance. In this approach, behavior of voltage depending resistance and capacity is traced. The data we obtained is plotted in figures 13-15. At a voltage of ~100 mV the specimen has a high polarization resistance and the capacity is at a minimum of 0 mV, which explains the good properties of the specimen in the 0-100 mV range, and its corrosion resistance on higher voltages. The capacity decreases for the interval: $E \in (-500 \text{ mV}, 0 \text{ mV})$ and then increases for the interval $E \in (0 \text{ mV}, 500 \text{ mV})$.

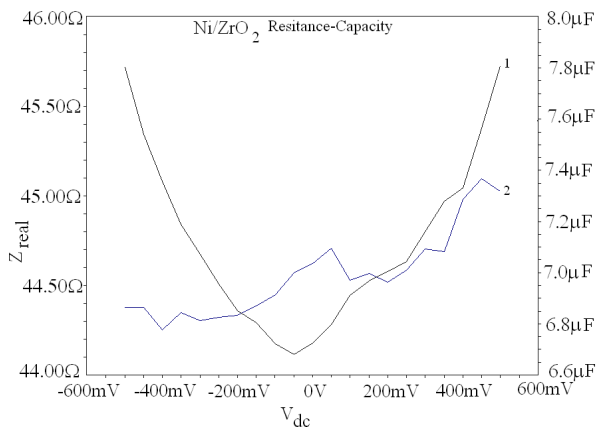


Fig.13. Variation of capacity (1) and resistance (2) of nanocomposite thin films versus applied potential.

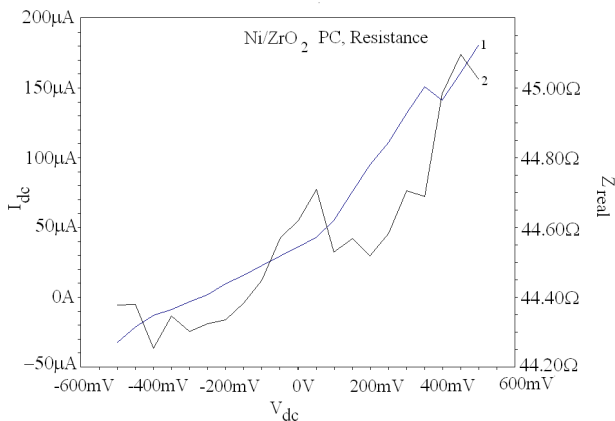


Fig.14. Polarization curve (1) and variation of resistance (2) of nanocomposite thin films.

Our experiments have shown that the Ni/ZrO₂ composite coatings resist better to corrosion, compared to metallurgical nickel depositions. The best corrosion protection is obtained when the layers have low capacity. The layer is less active, therefore more resistant to corrosion.

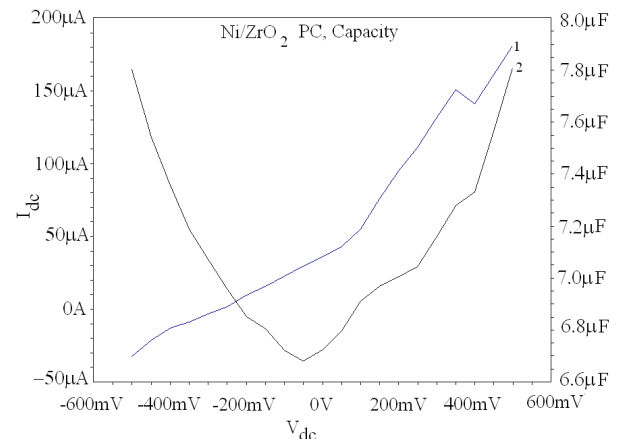


Fig.15 Polarization curve (1) and variation of capacity (2) of nanocomposite thin films

The specimens subjected to electrochemical studies were washed with plenty of distilled water and dried, and the rayon was subsequently removed from the coated surface [8, 9]. The specimens can be inspected with an electronic microscope to view potential alterations of the surface to be studied.

5. Conclusions

This paper deals with the electrochemical preparation and study of Ni/Al₂O₃ and Ni/ZrO₂ nanocomposite thin layers on Inconel or copper substratum. The comparison between the properties of composite coatings and metallurgical nickel coatings yielded conclusive results. Electrochemical processes offer an alternative way for obtaining composite coatings with unique properties, superior to those of constituent materials.

More than that, the composite coatings can be obtained using affordable processes which offer precise control on its parameters. We determined the most relevant factors for the success of composite coatings with directed composition are the nature of constituents, and electrolyte and electrolysis conditions. For example, the chemical and physical reactions of Ni/ZrO₂ composite plating depend on the electrolyte, for each test solution used.

The study of polarization curves and electrochemical impedance offers useful information on the kinetics of chemical reactions on the electrode. The corrosion voltage has higher values for composite coatings of Ni/ZrO₂ in Na₂SO₄ 0.1 M solution, which is the most appropriate solution for studying the polarization curves. The 0.1 M Na₂SO₄ concentration has an appropriate conductivity for performing electrochemical tests.

The physical and chemical properties (hardness, stability, wear and chemical resistance) of composite coatings are superior to those obtained by conventional procedures and recommend their usage in electronics, medicine, engineering and anti-corrosion protection. Alumina and zirconia composite electrodepositions were

done in a nickel matrix, and the result exhibited higher corrosion resistance than that of pure nickel.

Additions of alumina nanoparticles with a particle size of 20 nm of 5 g/l and 10 g/l into nickel plating bath change the preferred growth direction of the electrodeposited nickel from $\langle 100 \rangle$ to $\langle 111 \rangle$. When alumina is added, the microstructure of nanocomposite coatings is different from that obtained using pure nickel. Moreover, deposition of zirconia in nickel metallic matrix improves anti-corrosion protection of layers.

The obtained results are promising for developing new corrosion-resistant materials. They suggest that metal oxide nanoparticles coatings can be an effective option for surface protection, as it introduces a barrier against aggressive environment and metallic sub-layer. This approach is relatively new and warrants further research into the mechanisms that cause nickel-metal oxide composite coatings to improve corrosion resistance.

Acknowledgement

The authors thanks for the support of this work to T. Lempke and S. Steinhauser from Chemnitz University, Germany, and to C. Radovici and R. Banu from UPB Bucharest, as well as to G. Carac from Dunarea de Jos of Galati, Romania.

References

- [1] C. M. Abreu, M. J. Cristobal, R. Loada, X. R. Novoa, G. Pena, M. C. Perez, *Electrochem. Acta*, **51**, 2991(2006).
- [2] B-Y Yoo, R. K. Hendricks, M. Ozkan, N.V. Myung, *Electrochem. Acta*, **51**, 3543 (2006).
- [3] V. Viswanathan, A. Agarwal, V. Ocelik, J.T.M. De Hossom, N.Sobczak, S. Seal, *J. Nanosci Nanotechnol.* **6**, 651(2006).
- [4] Y. Leng, Y. Zhang, T. Liu, M. Suzuki, X. Li, *Nanotechnology*, **17**, 1797 (2006).
- [5] C. Gheorghies, C. Carac, I. V. Stasi, *J. Optoelectron. Adv. Mater.*, **8**, 1234 (2006).
- [6] C. H. Hamann, A. Hamnett, W. Vielstich, *Electrochemistry*, Ed. Wiley – VCH, Weinheim (1998).
- [7] D. R. Crow, *Principles and Applications of Electrochemistry* (Fourth Edition), Ed. Chapman & Hall, New York – London (1994).
- [8] P. H. Rieger, *Electrochemistry* (Second Edition), Ed. Chapman & Hall, New York -London, (1994).
- [9] C. M. A. Brett, A. M. Oliveira Brett, *Electrochemistry-Principles, Methods and Applications*, Ed. Oxford University Press, Oxford (1996).

*Corresponding author: cgheorg@ugal.ro